

# Measurement of the quadratic slope parameter in the $K_L \rightarrow 3\pi^0$ decay Dalitz plot

NA48 Collaboration

A. Lai, D. Marras, L. Musa

*Dipartimento di Fisica dell'Università e Sezione dell'INFN di Cagliari, I-09100 Cagliari, Italy*

A. Bevan, R.S. Dosanjh, T.J. Gershon<sup>1</sup>, B. Hay<sup>2</sup>, G.E. Kalmus<sup>3</sup>, D.J. Munday,  
M.D. Needham<sup>4</sup>, E. Olaiya, M.A. Parker, T.O. White, S.A. Wotton

*Cavendish Laboratory, University of Cambridge, Cambridge, CB3 0HE, UK<sup>5</sup>*

G. Barr, H. Blümer, G. Bocquet, A. Ceccucci, D. Cundy, G. D'Agostini, N. Doble,  
V. Falaleev, L. Gatignon, A. Gonidec, G. Govi, P. Grafström, W. Kubischta, A. Lacourt,  
M. Lenti<sup>6</sup>, S. Luitz<sup>7</sup>, J.P. Matheys, A. Norton, S. Palestini, B. Panzer-Steindel,  
G. Tatishvili<sup>8</sup>, H. Taureg, M. Velasco, H. Wahl

*CERN, CH-1211 Geneva 23, Switzerland*

C. Cheshkov<sup>\*</sup>, P. Hristov<sup>2</sup>, V. Kekelidze, D. Madigojine, N. Molokanova,  
Yu. Potrebenikov, A. Zinchenko

*Joint Institute for Nuclear Research, Dubna, Russian Federation*

I. Knowles, C. Lazzeroni, V. Martin, H. Parsons, R. Sacco, A. Walker

*Department of Physics and Astronomy, University of Edinburgh, JCMB King's Buildings, Mayfield Road, Edinburgh, EH9 3JZ, UK*

M. Contalbrigo, P. Dalpiaz, J. Duclos, P.L. Frabetti, A. Gianoli, M. Martini, F. Petrucci,  
M. Savrié

*Dipartimento di Fisica dell'Università e Sezione dell'INFN di Ferrara, I-44100 Ferrara, Italy*

A. Bizzeti<sup>9</sup>, M. Calvetti, G. Collazuol, G. Graziani, E. Iacopini

*Dipartimento di Fisica dell'Università e Sezione dell'INFN di Firenze, I-50125 Firenze, Italy*

H.G. Becker, M. Eppard, H. Fox, K. Holtz, A. Kalter, K. Kleinknecht, U. Koch,  
L. Köpke, I. Pellmann, A. Peters, B. Renk, S.A. Schmidt, V. Schönharting, Y. Schué,  
R. Wanke, A. Winhart, M. Wittgen

*Institut für Physik, Universität Mainz, D-55099 Mainz, Germany<sup>10</sup>*

J.C. Chollet, S. Crépe, L. Fayard, L. Iconomidou-Fayard, J. Ocariz, G. Unal,  
I. Wingerter

*Laboratoire de l'Accélérateur Linéaire, IN2P3-CNRS, Université de Paris-Sud, 91898 Orsay, France*<sup>11</sup>

G. Anzivino, P. Cenci, E. Imbergamo, P. Lubrano, A. Mestvirishvili, A. Nappi,  
M. Pepe, M. Piccini

*Dipartimento di Fisica dell'Università e Sezione dell'INFN di Perugia, I-06100 Perugia, Italy*

R. Carosi, R. Casali, C. Cerri, M. Cirilli, F. Costantini, R. Fantechi, S. Giudici,  
B. Gorini<sup>2</sup>, I. Mannelli, G. Pierazzini, M. Sozzi

*Dipartimento di Fisica dell'Università, Scuola Normale Superiore e Sezione INFN di Pisa, I-56100 Pisa, Italy*

J.B. Cheze, J. Cogan, M. De Beer, P. Debu, A. Formica, R. Granier de Cassagnac,  
E. Mazzucato, B. Peyaud, R. Turlay, B. Vallage

*DSM/DAPNIA-CEA Saclay, F-91191 Gif-sur-Yvette Cedex, France*

I. Augustin, M. Bender, M. Holder, M. Ziolkowski

*Fachbereich Physik, Universität Siegen, D-57068 Siegen, Germany*<sup>12</sup>

R. Arcidiacono, C. Biino, F. Marchetto, E. Menichetti, N. Pastrone

*Dipartimento di Fisica Sperimentale dell'Università e Sezione dell'INFN di Torino, I-10125 Torino, Italy*

J. Nassalski, E. Rondio, M. Szleper, W. Wislicki, S. Wronka

*Soltan Institute for Nuclear Studies, Laboratory for High Energy Physics, PL-00-681 Warsaw, Poland*<sup>13</sup>

H. Dibon, G. Fischer, M. Jeitler, M. Markytan, I. Mikulec<sup>2</sup>, G. Neuhofer, M. Pernicka,  
A. Taurok

*Österreichische Akademie der Wissenschaften, Institut für Hochenergiephysik, A-1050 Wien, Austria*

Received 26 June 2001; accepted 3 July 2001

Editor: L. Montanet

\* Corresponding author.

*E-mail address:* cheshkov@sunse.jinr.ru (C. Cheshkov).

<sup>1</sup> Present address: High Energy Accelerator Research Organization (KEK), Tsukuba, Ibaraki, 305-0801, Japan.

<sup>2</sup> Present address: EP, CERN, CH-1211, Geneva 23, Switzerland.

<sup>3</sup> Based at Rutherford Appleton Laboratory, Chilton, Didcot, OX11 0QX, UK.

<sup>4</sup> Present address: NIKHEF, PO Box 41882, 1009 DB Amsterdam, The Netherlands.

<sup>5</sup> Funded by the UK Particle Physics and Astronomy Research Council.

<sup>6</sup> On leave from Sezione dell'INFN di Firenze, I-50125 Firenze, Italy.

<sup>7</sup> Present address: SLAC, Stanford, CA 94309, USA.

<sup>8</sup> Present address: Carnegie Mellon University, Pittsburgh, PA 15213, USA.

<sup>9</sup> Dipartimento di Fisica dell'Università di Modena e Reggio Emilia, via G. Campi 213/A I-41100 Modena, Italy.

<sup>10</sup> Funded by the German Federal Minister for Research and Technology (BMBF) under contract 7MZ18P(4)-TP2.

<sup>11</sup> Funded by Institut National de Physique des Particules et de Physique Nucléaire (IN2P3), France.

<sup>12</sup> Funded by the German Federal Minister for Research and Technology (BMBF) under contract 056SI74.

<sup>13</sup> Supported by the KBN under contract SPUB-M/CERN/P03/DZ210/2000 and computing resources of the Interdisciplinary Center for Mathematical and Computational Modeling of the University of Warsaw.

## Abstract

A value of  $(-6.1 \pm 0.9_{\text{stat}} \pm 0.5_{\text{syst}}) \times 10^{-3}$  is obtained for the quadratic slope parameter  $h$  in the  $K_L \rightarrow 3\pi^0$  decay Dalitz plot at the NA48 experiment at the CERN SPS. The result is based on  $14.7 \times 10^6$  fully reconstructed  $K_L \rightarrow 3\pi^0 \rightarrow 6\gamma$  decays. This is the most precise measurement of any of the Dalitz plot slope parameters in the charged and neutral kaon decays so far. © 2001 Published by Elsevier Science B.V. Open access under [CC BY license](#).

## 1. Introduction

The  $K \rightarrow 3\pi$  decays Dalitz plot distributions can be expanded in powers of Dalitz plot variables  $u$  and  $v$  [1]:

$$|M(u, v)|^2 \propto 1 + gu + jv + hu^2 + kv^2, \quad (1)$$

$$u = \frac{(s_3 - s_0)}{m_{\pi^+}^2}, \quad v = \frac{(s_1 - s_2)}{m_{\pi^+}^2},$$

$$s_0 = \frac{s_1 + s_2 + s_3}{3}, \quad s_i = (P_K - P_i)^2, \quad i = 1, 2, 3,$$

where  $P_K$  and  $P_i$  are the four-momenta of the decaying kaon and  $i$ th pion ( $i = 3$  for the “odd charge” pion), respectively.

In the case of the  $K_L \rightarrow 3\pi^0$  decay the expression (1) reduces to [2]:

$$|M_{000}(R^2, \theta)|^2 \propto 1 + hR^2, \quad (2)$$

$$R^2 = (u^2 + v^2/3), \quad \theta = \arctan(v/\sqrt{3}u)$$

because of the identical final state particles. A positive/negative value of the quadratic slope parameter  $h$  would mean that asymmetric/symmetric final states are favoured.

Based only on isospin symmetry and some general assumptions it is possible to define a relation

$$\rho \equiv h + 3k - \frac{g^2}{4\cos^2\beta} \quad (3)$$

between the quadratic  $h$ ,  $k$  and linear  $g$  Dalitz plot slope parameters and the final-state interaction phases  $\beta$  which should be approximately the same for all  $K \rightarrow 3\pi$  decays [3]. For  $K_L \rightarrow 3\pi^0$  decays the parameter  $\rho$  is equal to  $2 \times h$  ( $k \equiv h/3$ ) and is not influenced by radiative corrections since all the final state particles are neutral. Thus a high statistics measurement of the quadratic slope parameter in the  $K_L \rightarrow 3\pi^0$  decay Dalitz plot could establish strong constraints to the Dalitz plot slope parameters and f.s.i.

phases in other  $K \rightarrow 3\pi$  decays. Also, it could be useful in the evaluation of radiative corrections applied to  $K^\pm \rightarrow \pi^\pm\pi^\pm\pi^\mp$  and  $K_L \rightarrow \pi^+\pi^-\pi^0$  decays. On the other hand, by combining the  $K_L \rightarrow 3\pi^0$  decay Dalitz plot slope parameter  $h$  with the linear and quadratic slope parameters in the  $K^\pm \rightarrow \pi^\pm\pi^\pm\pi^\mp$  decay it is possible to probe the validity of the  $\Delta I = 1/2$  rule.

The  $K_L \rightarrow 3\pi^0$  Dalitz plot slope parameter  $h$  has been estimated in the framework of ChPT [4–6]. The analysis includes a nonzero  $\Delta I = 3/2$  amplitude in the quadratic term of the Dalitz plot expansion (1) by taking into account the next-to-leading  $O(p^4)$  corrections. The phenomenological coupling constants in the chiral Lagrangian are evaluated using a fit to the recent experimental data in both  $K \rightarrow 2\pi$  and  $K \rightarrow 3\pi$  decays.

In this Letter we present a measurement based upon a data set collected with the NA48 detector in 1998. The detector acceptance has been estimated using a detailed Monte Carlo (MC) simulation.

## 2. Detector setup and data taking

The NA48 experiment is dedicated to the measurement of direct CP violation in  $K_{L,S}^0 \rightarrow 2\pi$  decays. The  $K_L$  beam is produced by 450 GeV/c protons from the CERN SPS hitting a 2 mm diameter and 400 mm long beryllium target at a production angle of 2.4 mrad. Passing through a set of collimators, a  $\pm 0.15$  mrad divergent  $K_L$  beam enters the decay volume 126 m downstream of the target. The evacuated 89 m long decay volume is followed by a helium tank which contains four drift chambers of the charged particle spectrometer. After the tank a scintillator hodoscope, a liquid krypton electromagnetic calorimeter, a hadron calorimeter and muon veto counters are placed.

The liquid krypton calorimeter (LKr) is designed to measure the energy, position and timing of electromagnetic showers [7]. The 127 cm long detector consists of 13212 readout cells in a projective tower geometry which points to the middle of the decay volume. Each cell of  $2 \times 2 \text{ cm}^2$  cross section is made of copper-beryllium ribbons which are extended longitudinally in a  $\pm 48 \text{ mrad}$  accordion structure. The readout cells are contained in a cryostat filled with about 20 t liquid krypton at 121 K. The initial current induced on the copper-beryllium electrodes is measured by 80 ns FWHM and digitized by 40 MHz FADCs. For the 1998 data taking period, the energy and position resolutions of the calorimeter were determined to be:

$$\frac{\sigma(E)}{E} = \frac{(3.2 \pm 0.2)\%}{\sqrt{E}} \oplus \frac{(0.09 \pm 0.01)}{E} \oplus (0.42 \pm 0.05)\%, \quad (4)$$

$$\sigma(x) \simeq \sigma(y) \simeq \frac{0.4 \text{ cm}}{\sqrt{E}} \oplus 0.05 \text{ cm} \quad (5)$$

with  $E$  measured in GeV.

The time resolution was better than 300 ps for photons with energies above 20 GeV.

The energy nonlinearity in the calorimeter response was found to be less than  $1 \times 10^{-3}$  between 6 GeV and 100 GeV [8].

The LKr detector contains the so-called neutral hodoscope which is made of a 4 mm thick plane of scintillating fibres placed near the maximum of the e.m. shower development. The neutral hodoscope is used in the estimation of the main trigger inefficiency and for an additional measurement of the event time.

A description of the whole experimental setup can be found elsewhere [9].

The  $K_L \rightarrow 3\pi^0 \rightarrow 6\gamma$  data sample was acquired by three different triggers. The first one is the neutral  $2\pi^0$  trigger (NUT  $2\pi^0$ ) in which each 25 ns the calibrated analogue sums of  $2 \times 8$  LKr cells are used to construct 64-channel  $x$  and  $y$  projections of the energy deposited in the calorimeter [10]. Based on these projections the total deposited energy  $E_{\text{sum}}$ , the first and second moments of the  $x$  and  $y$  energy distributions, and the time of the energy peaks are computed. The centre-of-gravity COG of the event and

the longitudinal vertex position are reconstructed as:

$$\text{COG}^{\text{trig}} = \frac{\sqrt{M_{1,x}^2 + M_{1,y}^2}}{E_{\text{sum}}}, \quad (6)$$

$$z_{\text{vertex}}^{\text{trig}} = z_{\text{LKr}} - \frac{\sqrt{E_{\text{sum}}(M_{2,x} + M_{2,y}) - (M_{1,x}^2 + M_{1,y}^2)}}{m_K} \quad (7)$$

where  $M_{1,x}$ ,  $M_{1,y}$  and  $M_{2,x}$ ,  $M_{2,y}$  are the first and second moments of the energy deposition,  $z_{\text{LKr}}$  is the longitudinal position of the calorimeter and  $m_K$  is the nominal kaon mass.

The proper decay time  $\tau^{\text{trig}}$  from the beginning of the decay region (just after the final collimator) in units of the  $K_S$  lifetime  $\tau_S$  is derived taking into account calibration constants. The events are accepted by the NUT  $2\pi^0$  trigger if  $E_{\text{sum}} > 50 \text{ GeV}$ ,  $\text{COG}^{\text{trig}} < 15 \text{ cm}$  and  $\tau^{\text{trig}}/\tau_S < 5$ . In addition, less than 6 energy peaks within 13.5 ns in both the  $x$  and  $y$  projections are required.

The second trigger (NUT  $3\pi^0$ ) uses the same hardware chain as NUT  $2\pi^0$  trigger but is specially set-up to select  $3\pi^0$  events by applying no condition on the number of the energy peaks.

The third trigger (Nhodo) is based on the information from the neutral hodoscope. It requires a coincidence of signals from the upper and lower or the left and right parts of the calorimeter. In order to reduce the trigger output rates the Nhodo trigger and the NUT  $3\pi^0$  one were properly down-scaled.

### 3. Data analysis

The  $K_L \rightarrow 3\pi^0 \rightarrow 6\gamma$  events were selected from all events which met at least one of the trigger requirements. The selection criteria required 6 or more LKr clusters satisfying the following conditions:

- the energy of the cluster had to be between 3 GeV and 100 GeV;
- to avoid energy losses in the LKr, the distance from the cluster to the closest dead calorimeter cell was required to be greater than 2 cm and the cluster had to be more than 5 cm from the beam pipe and the outer edge of the calorimeter.

All possible combinations of 6 clusters which passed these requirements were considered. In addition, the following further selection criteria were applied on each combination:

- the distance between all cluster pairs had to be greater than 10 cm in order to avoid overlapping of the clusters;
- all 6 clusters had to lie within 5 ns from the average cluster time;
- the sum of the clusters energies had to exceed 60 GeV which is sufficiently far from the NUT  $2\pi^0$  and NUT  $3\pi^0$  trigger threshold of 50 GeV;
- the radial position of the center-of-gravity

$$COG = \frac{\sqrt{(\sum_{i=1}^6 E_i x_i)^2 + (\sum_{i=1}^6 E_i y_i)^2}}{\sum_{i=1}^6 E_i},$$

- where  $E_i$ ,  $x_i$ ,  $y_i$  are the energies and positions of the six selected clusters, had to be less than 10 cm;
- no additional clusters with an energy  $> 1.5$  GeV were allowed within  $\pm 3$  ns from the event time to minimize possible accidental effects.
- The longitudinal vertex positions were reconstructed analogous to (7):

$$z_{\text{vertex}} = z_{\text{LKr}} - \frac{\sqrt{\sum_{i=1}^6 \sum_{j>i}^6 E_i E_j [(x_i - x_j)^2 + (y_i - y_j)^2]}}{m_K} \quad (8)$$

where  $E_i$  and  $x_i$ ,  $y_i$  are the energies and positions of the six selected clusters.

For each combination the invariant masses  $m_1$ ,  $m_2$  and  $m_3$  of all 15 possible photon pairings were computed using  $z_{\text{vertex}}$ . By applying a  $\chi^2$  criteria, the combination and pairing most compatible with the hypothesis that  $m_1$ ,  $m_2$  and  $m_3$  are equal to the nominal  $\pi^0$  mass were picked.

To ensure the purity of the sample, events which had one or more reconstructed tracks in the spectrometer or more than one hit per plane in the third and fourth drift chambers were rejected.

To improve the resolution on the Dalitz plot variables  $R^2$  and  $\tan(\theta)$  and to reduce differences in the energy resolutions and nonlinearities between data and

MC which may bias the measurement of the quadratic slope parameter  $h$ , all the events were passed through a kinematical fitting procedure with constraints. Assuming the neutral kaon coming from the  $K_L$  target and a  $K \rightarrow 3\pi^0 \rightarrow 6\gamma$  decay the cluster energies and positions are adjusted to minimize

$$\chi_{\text{fit}}^2 = \sum_{i=1}^6 \frac{(E_i - E_i^{\text{fit}})^2}{\sigma(E_i)^2} + \sum_{i=1}^6 \frac{(x_i - x_i^{\text{fit}})^2}{\sigma(x_i)^2} + \sum_{i=1}^6 \frac{(y_i - y_i^{\text{fit}})^2}{\sigma(y_i)^2}, \quad (9)$$

where  $\sigma(E_i)$ ,  $\sigma(x_i)$ ,  $\sigma(y_i)$  are given by (4) and (5) and  $E_i^{\text{fit}}$ ,  $x_i^{\text{fit}}$ ,  $y_i^{\text{fit}}$  are the adjusted energies and positions of the photons as functions of the 15 decay parameters (the kaon energy, the vertex position, the three Euler angles of the decay plane in the kaon rest frame, the Dalitz plot variables  $R^2$  and  $\theta$  and the 2 angles of the  $\gamma$  directions for each of the decaying  $\pi^0$ s). While the effect of the kinematical fitting on the  $E_K$  and  $z_{\text{vertex}}$  resolutions was small, the  $R^2$  and  $\theta$  resolutions were improved significantly. In particular the RMS widths of  $(R^2 - R_{\text{true}}^2)$  and  $(\theta - \theta_{\text{true}})$  from  $8.8 \times 10^{-2}$  and 48 mrad became  $3.0 \times 10^{-2}$  and 31 mrad, respectively.

Finally a cut  $\chi_{\text{fit}}^2 < 8.5$  was applied to exclude the tails in the  $\chi_{\text{fit}}^2$  distribution which differ for data and MC.

The numbers of data and MC events which passed the selection criteria are presented in Table 1.

To estimate the quadratic slope parameter  $h$ , the  $R^2$  distribution for the data events was corrected for the detector acceptance. For this purpose about  $8 \times 10^8$  Monte Carlo events were generated with  $h = 0$ . Then the quadratic slope parameter  $h$  was evaluated by a linear fit to the ratio of the data and MC  $R^2$  distributions (Fig. 1). The fit was done separately

Table 1

The summary of the number of accepted events and the measured values of the Dalitz plot slope parameter  $h$  for the NUT  $3\pi^0$ , NUT  $2\pi^0$  and Nhodo triggers (the errors are statistical only)

	NUT $3\pi^0$	NUT $2\pi^0$	Nhodo
Data events	$12.43 \times 10^6$	$1.48 \times 10^6$	$0.82 \times 10^6$
MC events	$4.76 \times 10^6$	$4.53 \times 10^6$	$2.49 \times 10^6$
$h \times 10^3$	$-6.36 \pm 1.06$	$-4.49 \pm 1.88$	$-7.53 \pm 2.50$

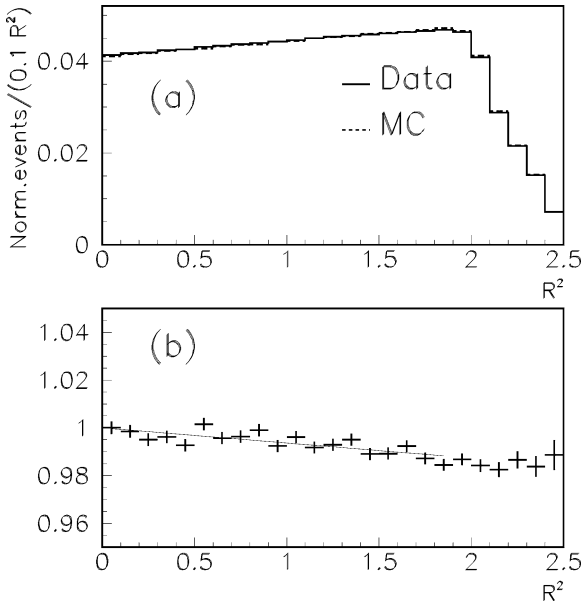


Fig. 1. (a) The data (solid line) and MC (dashed line)  $R^2$  distributions for the NUT  $3\pi^0$  trigger. (b) A linear fit to the normalized at  $R^2 = 0$  ratio of these distributions.

for each of the triggers using the corresponding MC samples within appropriate decay regions.

An important feature of the analysis was that the ratio of the data and MC  $R^2$  distributions was fitted up to 1.9 (Fig. 1). This allowed us to significantly improve the stability of the result by excluding the part of the Dalitz plot most affected by the energy resolution and nonlinearities. Since the shape of the detector acceptance on  $R^2$  depends mainly on the kaon energy, the whole analysis was done in kaon energy bins. Combining the measured values of the Dalitz plot slope parameter  $h$  presented in Fig. 2 and Table 1 we get a overall result of  $(-6.1 \pm 0.9) \times 10^{-3}$ .

#### 4. Systematics

Contributions of the detector acceptance estimation, the  $\chi^2_{\text{fit}}$  cut, the trigger conditions and the differences in the energy resolution, nonlinearities and energy scale between the data and MC to the systematic error were considered.

In order to study possible uncertainties in the acceptance we divided the data and MC samples upon the decay length  $\tau/\tau_s$ , the longitudinal vertex posi-

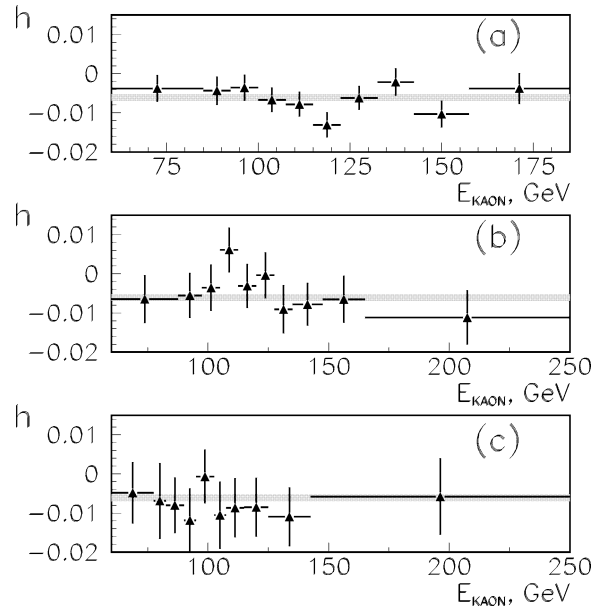


Fig. 2. The  $K_L \rightarrow 3\pi^0$  decay Dalitz plot slope parameter  $h$  in kaon energy bins for the NUT  $3\pi^0$  (a), NUT  $2\pi^0$  (b) and Nhodo (c) triggers, respectively. The overall result and the statistical error are shown by the shaded areas.

tion  $z_{\text{vertex}}$  and the centre-of-gravity COG. For each considered trigger sample the maximum deviation between the average value of  $h$  from Table 1 and the values obtained averaging over the dependence of a second variable ( $\tau/\tau_s$ ,  $z_{\text{vertex}}$ , COG) was taken as systematic error (Table 2).

An important check of the reliability of the MC was done by comparing the data and MC Dalitz plot

Table 2

The Dalitz plot slope parameter  $h$  in units of  $10^{-3}$  for the different subdivisions of the data and MC

	NUT $3\pi^0$	NUT $2\pi^0$	Nhodo
In $z_{\text{vertex}}$ bins	-6.50	-4.48	-6.72
$\chi^2/\text{n.d.f}$	14.3/9	7.4/10	6.9/10
In $\tau/\tau_s$ bins	-6.43	-4.58	-7.70
$\chi^2/\text{n.d.f}$	14.6/9	8.9/9	7.2/9
In COG bins	-6.38	-4.64	-7.56
$\chi^2/\text{n.d.f}$	12.4/9	11.6/9	5.7/9
$\Delta h$	0.14	0.16	1.0

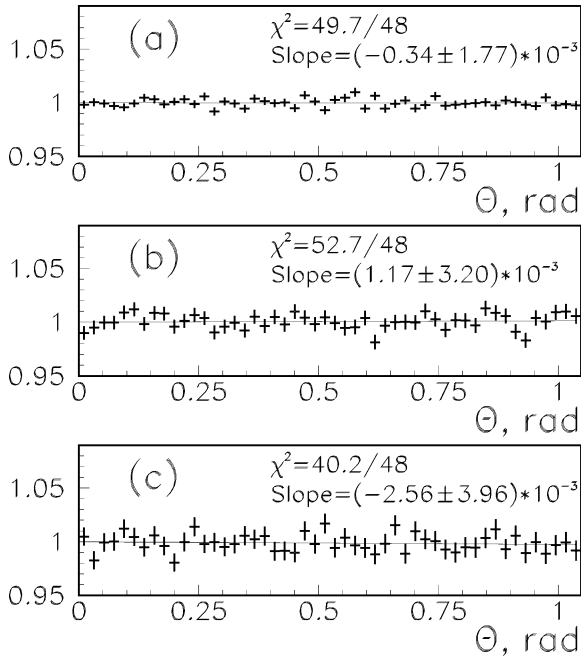


Fig. 3. The normalized ratios of the data and MC  $\theta$  distributions for the NUT  $3\pi^0$  (a), NUT  $2\pi^0$  (b) and Nhodo (c) triggers. The ratios were fitted with  $f(\theta) = (1 + \text{Slope} \times \theta)$ .

variable  $\theta$  (Fig. 3). A linear fit to the ratio of the data and MC  $\theta$  distributions clearly points to a very good agreement between experimental data and the simulation.

The second considered source of systematics was the difference between the data and MC cluster energy resolution. Using the measured and kinematically adjusted cluster energies we established a strong control over the resolutions seen in the data and the MC. The differences in the resolutions were adjusted by an additional smearing to the cluster energies in the MC. The maximum change in  $h$  after these adjustments was found to be  $\pm 0.20 \times 10^{-3}$  and was taken as a systematic error. A similar approach was applied in the study of the systematics due to the energy nonlinearities leading to a  $\pm 0.17 \times 10^{-3}$  systematic error on the  $h$ . To take into account small non-gaussian tails in the cluster energy resolution seen in the data, a simplified parameterization was used to add the tails to the MC events. The effect of the tails was found to be negligible. Changing the energy scale in the MC by  $\pm 1 \times 10^{-3}$  we got a shift in  $h$  of  $\pm 0.17 \times 10^{-3}$ .

The influence of the trigger conditions was studied by subdividing the data and MC in  $\tau/\tau_s$  bins. Although that for the NUT  $2\pi^0$  and Nhodo trigger samples no systematic effect was found, the result for NUT  $3\pi^0$  trigger sample was affected by a small NUT inefficient region near the  $\tau^{\text{trig}}/\tau_s$  cut. The data and MC were processed excluding this region and the change in the result of  $0.1 \times 10^{-3}$  gave us a systematic error due to the trigger.

The stability of the result upon the  $\chi^2_{\text{fit}}$  cut was checked by loosening it to 17. No statistically significant effect on  $h$  was established. Furthermore, the result was found to be stable upon different cuts on the clusters energies and positions in LKr.

No influence of a possible background contamination from  $\gamma$  conversions and Dalitz decays was observed.

All the sources of systematic error were added quadratically and yield a total systematic error of  $0.5 \times 10^{-3}$ .

In addition, a second independent analysis has been performed yielding a consistent result.

## 5. Conclusions

Our result for the Dalitz plot slope parameter in the  $K_L \rightarrow 3\pi^0$  decay is  $h = (-6.1 \pm 0.9_{\text{stat}} \pm 0.5_{\text{sys}}) \times 10^{-3}$ , where the errors are statistical and systematic, respectively. This result is in an agreement with the value of  $(-12 \pm 4) \times 10^{-3}$  predicted in [4]. The previous measurement of  $(-3.3 \pm 1.1_{\text{stat}} \pm 0.7_{\text{sys}}) \times 10^{-3}$  performed by the E731 experiment [11], is comparable with the result presented in this Letter.

## Acknowledgements

We would like to thank the technical staff of the participating laboratories, universities and affiliated computing centres for their support and cooperation.

## References

- [1] D. Groom et al., Review of Particle Physics, Eur. Phys. J. C 15 (2000) 1–878.
- [2] T. Devlin, J. Dickey, Rev. Mod. Phys. 51 (1979) 237.

- [3] A. Belkov et al., *Phys. Part. Nucl.* 26 (3) (1995) 239.
- [4] J. Kambor et al., *Phys. Rev. Lett.* 68 (1992) 1818.
- [5] J. Kambor et al., *Phys. Lett. B* 261 (1991) 496.
- [6] G. D'Ambrosio et al., *Phys. Rev. D* 50 (1994) 5767.
- [7] G. Barr et al., *Nucl. Instrum. Methods A* 370 (1996) 413.
- [8] G. Unal for the NA48 Collaboration, Talk on 9th Int. Conf. on Calorimetry in Particle Physics, 9–14 October 2000, hep-ex/0012011.
- [9] V. Fanti et al., *Phys. Lett. B* 458 (1999) 553.
- [10] G. Fischer et al., *Nucl. Instrum. Methods A* 419 (1998) 695.
- [11] S. Somalwar et al., *Phys. Rev. Lett.* 68 (1992) 2580.